HHS Public Access

Author manuscript

Proc Inst Mech Eng H. Author manuscript; available in PMC 2024 December 02.

Published in final edited form as:

Proc Inst Mech Eng H. 2024 June ; 238(6): 608–618. doi:10.1177/09544119241264304.

Optimization of activity-driven event detection for long-term ambulatory urodynamics

Farhath Zareen[1], **Mohammed Elazab**[2], **Brett Hanzlicek**[3], **Adam Doelman**[2,4], **Dennis Bourbeau**[3,5], **Steve JA Majerus**[3,6], **Margot S Damaser**[2,3], **Robert Karam**[1]

[1]Department of Computer Science and Engineering, University of South Florida, Tampa, FL, USA

[2]Department of Biomedical Engineering, Lerner Research Institute, Cleveland Clinic, Cleveland, OH, USA

[3]Research Service, Louis Stokes Cleveland VA Medical Center, Cleveland, OH, USA

[4]International Collaboration on Repair Discoveries, University of British Columbia, Vancouver, BC, Canada

[5]Department of Physical Medicine and Rehabilitation, MetroHealth System, Cleveland, OH, USA

[6]Department of Electrical, Computer, and Systems Engineering, Case Western Reserve University, Cleveland, OH, USA

Abstract

Lower urinary tract dysfunction (LUTD) is a debilitating condition that affects millions of individuals worldwide, greatly diminishing their quality of life. The use of wireless, catheter-free implantable devices for long-term ambulatory bladder monitoring, combined with a single-sensor system capable of detecting various bladder events, has the potential to significantly enhance the diagnosis and treatment of LUTD. However, these systems produce large amounts of bladder data that may contain physiological noise in the pressure signals caused by motion artifacts and sudden movements, such as coughing or laughing, potentially leading to false positives during bladder event classification and inaccurate diagnosis/treatment. Integration of activity recognition (AR) can improve classification accuracy, provide context regarding patient activity, and detect motion artifacts by identifying contractions that may result from patient movement. This work investigates the utility of including data from inertial measurement units (IMUs) in the classification pipeline, and considers various digital signal processing (DSP) and machine learning (ML) techniques for optimization and activity classification. In a case study, we analyze simultaneous bladder pressure and IMU data collected from an ambulating female Yucatan minipig. We identified 10 important, yet relatively inexpensive to compute signal features, with which we achieve an average 91.5% activity classification accuracy. Moreover, when classified activities are included in the bladder event analysis pipeline, we observe an improvement in classification accuracy, from 81% to

Corresponding author: Robert Karam, Department of Computer Science and Engineering, University of South Florida, 4202 E. Fowler Ave, Tampa, FL 33620-9951, USA. rkaram@usf.edu.

Declaration of conflicting interests

The author(s) declared no potential conflicts of interest with respect to the research, authorship, and/or publication of this article.

89.0%. These results suggest that certain IMU features can improve bladder event classification accuracy with low computational overhead.

Clinical Relevance: This work establishes that activity recognition may be used in conjunction with single-channel bladder event detection systems to distinguish between contractions and motion artifacts for reducing the incorrect classification of bladder events. This is relevant for emerging sensors that measure intravesical pressure alone or for data analysis of bladder pressure in ambulatory subjects that contain significant abdominal pressure artifacts.

Keywords

Ambulatory urodynamic monitoring; activity recognition; feature optimization; bladder event detection

Introduction

Urodynamic studies (UDS) are the gold standard for diagnosing and managing Lower Urinary Tract Dysfunction (LUTD). These studies utilize multiple catheters and create artificial test conditions to assess bladder function. Specifically, the bladder is retrogradely filled with saline at superphysiological infusion rates. Typically, two catheters are used: an intraurethral catheter to measure intravesical pressure (P_{ves}) and a rectal balloon catheter to measure abdominal pressure (P_{abd}). Detrusor pressure (P_{det}) is computed by finding the simultaneous difference between vesical and abdominal pressure, which is then used to distinguish between bladder contraction events and abdominal-induced increases in P_{ves}. However, due to the high infusion rates and the dual-sensor system, UDS can be susceptible to artifacts, potentially leading to diagnostic inaccuracies.[1,2] The use of wireless, catheter-free implantable devices can enable long-term ambulatory bladder monitoring during natural filling to enhance the diagnosis of LUTD. Recently published works have demonstrated significant progress toward developing wireless sensors to enable long-term ambulatory UDS.[3–5] However, it is expected that extended ambulatory bladder monitoring will generate large datasets of pressure recordings spanning days or weeks, and this single-sensor data will include P_{abd} and contributors to P_{ves} other than P_{det}.

For treatment, neuromodulation via electrical stimulation can increase bladder capacity[6] and is a potential solution after the failure of more conservative approaches.[7] However, conditional stimulation requires sensory feedback to determine bladder activity and for accurate stimulation, bladder events must be detected near the onset of a contraction. State-of-the-art research is investigating conditional neurostimulation using wireless sensors in clinical settings.[8–11] Prior work in bladder event detection for conditional stimulation has demonstrated the feasibility of distinguishing between bladder contractions and abdominal artifacts arising from movement such as coughs, laughs, sneezes, etc., in the clinical setting.[12] However, real-time conditional stimulation in ambulatory settings presents additional challenges since long-term sensor data will contain physiological noise caused by patient movement in addition to other sensor noise.

To tackle these diagnostic and treatment challenges, one potential solution is to monitor and classify patient activity in tandem with bladder pressure. While this results in significant

additional data for processing, it provides important context for the bladder activity. Integrating patient activity with an event detection system may improve the classification of bladder events by distinguishing between true contractions and motion artifacts. However, typical activity recognition (AR) systems incur large computational overheads, making their integration with low-power mobile devices impractical. In this work, we aim to reduce the computational burden associated with activity recognition AR through the use of digital signal processing (DSP) and machine learning (ML) techniques, then integrate the activity recognition AR into a bladder event detection algorithm for single-channel systems. We begin with a popular human activity recognition (HAR) dataset[13] and apply various optimization techniques, leading to a significant reduction in the computational overhead while maintaining acceptable activity classification accuracy. Finally, we perform a case study on simultaneous bladder pressure and inertial data collected from an ambulating female Yucatan minipig to test the performance of the optimized AR and its integration with a bladder event detection system. Specifically, we present the following contributions:

1. We utilize the HAR dataset to refine the feature space and reduce computational complexity while minimally impacting the activity classification accuracy.
2. We develop and implement a sensor fusion algorithm to integrate activities classified from inertial features with simultaneous bladder pressure recordings in real time.
3. We evaluate our approach on an ambulating Yucatan minipig and demonstrate an improvement in bladder event detection accuracy.

The rest of the paper is organized as follows: Section “Background” presents the background on ambulatory urodynamic monitoring and AR. Section “Methodology” discusses the methodology where optimization techniques to reduce the computational costs of implementing AR are presented, along with a case study utilizing the pig dataset. It also presents the integration of the activity data with a bladder event detection system to identify motion artifacts. Section “Results” delves into the results where the optimized AR is assessed on the HAR and pig datasets. The bladder event detection system with integrated activity data is also evaluated. We discuss the results in context with related work in Section “Discussion” and conclude with future work in Section “Conclusion.”

Background

Ambulatory urodynamic monitoring and treatment

In clinical UDS procedures, two separate catheter-based sensors are used, one measuring bladder pressure P_{ves}, and the other measuring abdominal pressure P_{abd}. Detrusor pressure P_{det} generated from bladder contractions is then obtained by computing the simultaneous difference between P_{ves} and P_{abd}, as shown in equation (1).

$$P_{det} = P_{ves} - P_{abd} \tag{1}$$

Catheter-based measurements make long-term bladder monitoring impractical, and even short-term monitoring during ambulation is difficult. As such, current options for treatment through electrical stimulation are limited to open-loop modalities. Devices like the InterStim Implantable Stimulator (Medtronic) have been employed to manage conditions such as overactive bladder by delivering continuous stimulation to the sacral nerve.[14,15] Conditional neuromodulation can also inhibit unwanted bladder contractions or address feelings of urgency while reducing the risk of habituation and conserving battery life.[16] However, for effective stimulation in closed-loop neuromodulation, contractions must be detected near onset, typically within seconds. Such an approach therefore requires real-time feedback on bladder activity.

In general, many of the challenges associated with ambulatory bladder monitoring can be addressed through the use of wireless *implanted* sensors. Numerous recent studies propose the use of wireless implanted sensors to provide long-term measurement data during natural filling.[5,8,17–20] Others have noted that a wireless implant, paired with a smart algorithm (either in the implant, or else in the external receiver to which the implant transmits measurement data), can enable personalized, closed-loop treatment of UDS.[8,9,21,22]

However, long-term monitoring and conditional neuromodulation come with their own set of challenges:(1) long-term monitoring will result in very large and potentially noisy datasets, and (2) without a second sensor, the measured pressure will contain artifacts from P_{abd} which may confound a closed-loop control system. For diagnosis, inspecting days, weeks, or months worth of noisy data is impractical; for treatment, closed-loop neuromodulation would require a method to either (1) estimate detrusor pressure from bladder pressure and/or (2) detect true bladder contraction events in the presence of significant physiological noise. While existing work in bladder pressure signal analysis has demonstrated effective techniques for accurately detecting bladder events in real-time using P_{ves}, this was done in clinical settings[23,24] with limited physiological noise, and few abdominal artifacts. Real-world conditions are far more variable.

In this paper, we propose the use of a second, worn sensor—an inertial measurement unit (IMU)—to provide additional context for the measured bladder pressure signal. The additional context can be utilized, for example, in classifying the individual's current movements as a particular activity. This can enable more accurate characterization of bladder events in long-term data, and also be used by a control algorithm when deciding whether or not to trigger stimulation.

Activity recognition and feature optimization

AR aims to interpret movement by analyzing sensory data obtained from interactions with the environment. Sensors such as accelerometers and gyroscopes, which are commonly used for tracking body movement and orientation, detect changes in motion and measure angular velocity and rotation, respectively. These sensors can be built on a single chip and can be found in several commercial electronic devices.[25–27] This is the case with IMUs, which are widely used in HAR as they are wearable and long-lasting autonomous devices.[28–31] By analyzing the data from these sensors, AR systems can identify and classify various basic and dynamic activities. Recently, several research groups have established benchmark

datasets for AR by simulating real-life scenarios, variabilities, and activities.[13,32–34] They serve as a standard reference point for ML models trained in recognizing various activities from accelerometry or gyroscopic features. In the context of bladder event detection, human activity can provide additional context about what the individual was doing at the time, which may affect the bladder pressure. For example, running may result in changes in bladder pressure due to the contribution of abdominal muscles; conversely, while at rest, an increase in bladder pressure is more likely to be due to the detrusor muscle contracting. The use of IMU data for contextualization of bladder pressure is compelling, particularly if it can improve bladder event detection accuracy.

However, AR systems generally have high computational complexity and this kind of sensor data generates massive amounts of unlabeled data, which may make meaningful feature extraction more difficult and hinder accurate activity classification. Moreover, the feature extraction cost typically dominates the test-time runtime cost in AR implementations.[35,36] Processing a large number of features requires more computational resources and can result in slower execution times. As shown in Table 1, the cost of computing features (indicated very low, low, medium, and high) can vary in complexity and should be considered, especially for on-chip AR. Most time-domain features such as mean and standard deviation require limited operations that have a linear relation to the number of input samples n, and these operations are typically arithmetic additions and subtractions. While some features may exhibit a linear relationship between operations and input samples that include multiplications and divisions, there may also be features that are quadratic, increasing the computational cost. Along with cost, storage, and memory operations should also be considered to store temporary variables in addition to storing the input signal data. Additionally, frequency-domain features are computationally more expensive than time-domain features as they require a Fast Fourier Transform (FFT) to be performed. For example, in this work, we utilize a dataset from[13] that consists of 561 time and frequency domain features such as mean, standard deviation, kurtosis, skewness, correlation, energy, entropy, etc. The features are computed for signal “windows” which consist of n samples (e.g., $n = 256$, representing2.56 s worth of data at a 100 Hz sample rate), in order to form a *feature vector*. Moreover, windows may overlap, for example, the first window may go from time $t = 0$ to $t = 256$, and the second may go from $t = 128$ to $t = 384$, and so on. Each feature vector is input to an ML classifier, which then processes and classifies it. In the case of AR, these classes may be walking, running, or other activities the classifier has been trained to recognize.

ML techniques such as random forests (RF), Gaussian Naïve Bayes (GNB), and logistic regression (LR) have been employed in the context of AR to analyze raw sensor signals and build large feature sets for activity classification.[37–39] Both GNB and LR are attractive classifiers for AR as they can handle high-dimensional data such as sensor data from wearable devices or monitoring systems efficiently. They can be applied to real-time classification and can be extended to handle multi-class classification, which is important for AR. Feature reduction techniques can be employed to optimize large feature space and reduce computational complexity by selecting a subset of the most discriminative features or by transforming the original features into a lower-dimensional representation. In this work, we explore principal component analysis (PCA),[40] random forest (RF) feature importance,[41]

and random projections (RP)[40] to optimize the feature set and compare ML classifiers GNB and LR for activity classification.

Methodology

The primary objectives of this work are: (1) to optimize the feature space to reduce the overall computational overhead of AR implementation with minimal loss in accuracy, and (2) to integrate the generated activity data with simultaneous bladder pressure data, enhancing bladder event detection. Specifically, we first used the HAR dataset to evaluate three feature space reduction methodologies. In addition, we explored three sample rates —the original, 100 Hz, and two filtered and downsampled rates of 50 and 25 Hz, in an effort to optimize the activity classification process. We then conducted a case study on an ambulating Yucatan minipig in which an implantable bladder pressure monitor, the Urological Monitor of Conscious Activity (UroMOCA) device—had been implanted. The UroMOCA provided P_{ves}, while a worn IMU provided simultaneous accelerometry and gyroscopic data. This was then assessed with the optimized AR framework. Finally, the classified activities were input, along with the bladder pressure, to a bladder event detection algorithm, allowing us to evaluate the effect of incorporating activity classes on bladder event classification accuracy. The following subsections provide additional details on each step of the methodology.

Optimizing the activity recognition process

HAR dataset.—The HAR dataset consists of experiments conducted on 30 participants aged between 19 and 48 years. Each participant performed basic activities such as walking, sitting, standing, and lying while wearing a Samsung Galaxy S II smartphone on their waist. The smartphone's built-in accelerometer and gyroscope recorded three-dimensional linear acceleration and angular velocity sampled at 100 Hz. These experiments were captured on video to aid in manual data labeling and the dataset was randomly divided into 70% training and the remaining 30% for testing. The recorded signals were processed from the accelerometer and gyroscope by filtering out noise and segmented into 2.56-second sliding windows, each overlapping the next by 50%. The acceleration data, containing both gravitational and body movement elements, was divided using a Butterworth low-pass filter with a cutoff frequency $f_c = 0.3$ Hz. This split the data into components of body acceleration and gravitational forces. For every window, a feature vector was derived by analyzing aspects in both the time and frequency domain. A total of 561 time and frequency domain features were obtained. This dataset is described in detail in Anguita et al.[13] and is freely available.

Feature optimization for HAR.—To optimize the HAR dataset, we utilized PCA, RF feature importance, and RP to obtain the most important features from the large feature space. Moreover, computationally dependent features were identified to avoid redundant recomputation. We then compared ML classifiers GNB and LR for activity classification.

Case study on pig data for bladder event classification

Pig dataset.—In vivo procedures were approved by the Institutional Animal Care and Use Committee (IACUC) of the Cleveland Clinic, Cleveland, OH. Data were collected using the UroMOCA device that wirelessly measures bladder pressure and volume without catheters.[4] The subject involved in this study was a female Yucatan minipig. The UroMOCA was surgically implanted via laparotomy and cystotomy under anesthesia. The bladder capacity of the subject was determined using gravity filling before UroMOCA implantation. Baseline cystometry was performed using a 5-fr dual lumen catheter while saline was infused at 20 mL/min to measure P_{ves}. After recovery from implantation, pressure and volume were recorded for at least 3 h per session while the subject was awake and untethered. Following 2 weeks of UroMOCA implantation, device functionality was assessed via cystometry and saline bolus infusions while the subject was anesthetized. Two weeks later, after additional conscious ambulatory recordings, the subject was euthanized. This work utilized a total of five recordings from the pig dataset sampled at 100 Hz, across three different days, consisting of at least 3 h of recorded bladder pressure and volume data. Acceleration and gyroscope data were captured using the SparkFun OpenLog Artemis, an open-source data logger with a built-in logging feature for the triple-axis accelerometer and gyroscope. This data logger was inserted into a pocket on a vest worn by the pig. For this study, the accelerometer and gyroscope recordings were sampled at 100 Hz to align with the HAR dataset, and the UroMOCA data collection rate. To validate the IMU readings, manual annotations were recorded, detailing the pig's observed activities including voiding events. These annotations were subsequently used to confirm accuracy of the sensor data, ensuring that the IMU measurements precisely reflected the actual movements of the pig. The overall data processing methodology is outlined in Figure 1.

Activity recognition and classification.—Movement data were collected from the OpenLog Artemis datalogger/IMU's built-in triaxial accelerometer and gyroscope. A fifth order median filter was initially applied for denoizing. A 0.3 Hz cutoff frequency was used to separate body and gravity components from the signals. Fixed-width windows of 256 samples, overlapping by 50%, were processed. All 561 features were initially computed for each of these 256 sample windows, as described in Anguita et al.[13,42] We then evaluated the performance of PCA, RF feature importance, and RP in conjunction with ML classifiers to optimize the AR procedure. Once the most important features were identified, GNB and LR were evaluated for activity classification. Training and testing were performed in a random 70–30 split. Based on our experiments, we found that RF feature importance, combined with the LR classifier, was able to identify the 10 most discriminative features, out of 561 total features, and then use those limited features to maximize activity classification accuracy. The experiments were repeated after downsampling the IMU signals to 50 and 25 Hz, to further reduce the overall computational overhead by 50% or 75%, respectively. To evaluate the performance of the AR system, the following metrics were measured: (1) Accuracy, which measures the number of samples correctly predicted to the total number of samples; (2) F1-score, computed as the harmonic mean of precision and recall. While the accuracy metric is provided, F1 is preferred in this context due to the imbalance in class sizes. The metrics are described in detail below:

$$\text{Accuracy} = \frac{TP + TN}{TP + TN + FP + FN} \tag{2}$$

$$\text{Precision} = \frac{TP}{TP + FP} \tag{3}$$

$$\text{Recall} = \frac{TP}{TP + FN} \tag{4}$$

$$\text{F1} - \text{score} = \frac{2 * Precision * Recall}{Precision + Recall} \tag{5}$$

After detecting activities, the corresponding activity IDs and their timestamps were integrated into the bladder event detection framework to evaluate multimodal sensor fusion in bladder event classification.

Bladder event classification.—The event detection algorithm utilized single-sensor P_{ves} to detect bladder events, including contractions and other abdominal-induced artifacts. A series of processing stages were used to distinguish pressure caused by P_{det} from that caused by P_{abd}. These stages involved initial filtering, wavelet transformation, and adaptive thresholding.[23] The signal was first filtered to eliminate noise using an exponential moving average (EMA) filter, with a low-pass cutoff frequency of 0.1 Hz. A multi-level wavelet transform was then applied to the filtered output, where the Daubechies 4-tap wavelet was used as the basis function. The output included approximation and detail coefficients, where the approximation coefficients reflected the signal's general trend, while the detail coefficients represented abdominal artifacts and other sensor noise. Maximum pressure peaks were identified in the signal to account for changes in pressure. An adaptive thresholding approach in the wavelet space was then used. A user-selectable percentile, for example, 90th, was selected. Samples in the wavelet space were sorted in rank order. In the next window, a transformed sample exceeding this threshold, typically a high-pressure event, was categorized as a bladder contraction.[23] First, these pressure-only detected bladder events were evaluated. Then, the output activity IDs and timestamps from the AR pipeline were integrated into the bladder event detection system to validate the detected bladder events. The specific way in which AR can impact bladder event detection can potentially vary; for example, contractions detected during a "run" (RN) event may be categorized one way, while contractions detected during a "stand/stationary" (ST) activity may be categorized another way. For the purpose of our experiments, bladder events detected during an activity period (WK, RN) were considered to be motion artifacts (false positives).

Results

Feature optimization on HAR dataset

We first utilized the HAR dataset to evaluate the different feature reduction techniques in conjunction with signal processing and ML classifiers to optimize activity classification. The feature space from the HAR dataset consisted of 561 features where the original classification accuracy was 96%. As previously stated, computing all 561 features consumes significant computational resources. Table 2 shows classification results when using only the 50 most important features, as identified by PCA, RF, and RP. We found that features identified by RF used in conjunction with the LR classifier achieved a detection accuracy of 93.9%, a 91.0% decrease in the feature space costing a 2.2% decrease in activity classification accuracy. In general, this approach may be applied iteratively in a design space exploration to find a subset of n features for which the resulting accuracy loss is within acceptable bounds.

Application to the pig dataset

We applied these optimization techniques (LR in conjunction with the RF feature importance) to the IMU data collected from the pig subject. Across all trials, we achieved an average 91.5% classification accuracy using a feature subset of 10 features for data down-sampled to 50 Hz, which resulted in a 98.2% reduction in the feature space, with a 4.8% reduction in activity classification accuracy. The results of classification accuracy after applying the optimization techniques for varying F_s are shown in Table 3. Table 4 shows the confusion matrix of all the detected activities in the pig dataset. The trade-off between prediction accuracy and cost could be viewed in terms of portability cost for *on-board* classification of activities. In resource-constrained wearable and implantable medical devices, the computational and memory costs of handling a large feature space can impact power consumption, execution times, and overall device size. Therefore, while there is a decrease in accuracy, the optimizations to the feature space reduced significant computational demands to allow for more practical and efficient deployment of the model, paving the way for eventual on-board activity classification. To evaluate the significance of individual features, we ran feature importance across all trials over 20 iterations. This allowed us to compute the mean importance of each feature and utilize this ranking to consistently identify the most important features. Figure 2 shows the top 15 identified features. The figure illustrates the results of employing RF feature importance to identify features for activity classification, where the x-axis denotes the calculated "feature importance," a numerical indicator of each feature's relative contribution to the model's predictive accuracy. The higher the value, the more critical the feature is deemed. The y-axis lists the top 15 features, with those prefixed by "t" extracted from the time domain (TD), representing raw and statistical measures over time, and those prefixed by "f" from the frequency domain (FD), encapsulating the distribution and intensity of the signal. For example, time-domain features such as *t_body_acc_jerk_Mean*(), capture statistics like the rate of change in acceleration, which can be directly observed over time, whereas, frequency-domain features like *f_body_acc_Mag_energy*(), offer insight into periodic motion characteristics, crucial for detecting repetitive activities. The top identified features include signal magnitude area (sma) of body acceleration, maximum (max) value

of body acceleration, standard deviation (std) of the magnitude of body acceleration, interquartile range (iqr), etc.

Bladder event classification

In this study, “Experiments” (exp) refers to distinct days on which data was collected, while “Trials” denotes the individual recording sessions. To account for motion artifacts in the recordings, the output activity IDs and timestamps from the optimized AR framework were integrated with the bladder event detection system. The time signals were synchronized, and changes in pressure with respect to motion artifacts were assessed. The detected events were validated against annotated notes consisting of voiding events, which constituted our ground truth. These annotations also included detailed timestamps corresponding to the activities performed by the pig subject. In Figure 3, bladder events from two experiments in the pig dataset are depicted. Events detected were differentiated based on true bladder contractions and abdominal artifacts. In this work, we used the terms correctly classified and incorrectly classified to describe true positive (TP)/true negative (TN) rates and false positive (FP)/false negative rates (FN), respectively. The results of the bladder event detection system are shown in Table 5 where total detected events were the events detected before activity validation and valid events were the events verified after activity integration. Across all the trials, the average correctly classified before activity validation was 81%. To account for motion artifacts, activity data was integrated into the bladder event detection system highlighting different activity regions. Contractions found during activity periods were considered incorrectly classified events and were invalidated, which improved the bladder event classification to 89%. By integrating an additional sensor to monitor motion activity, the system’s ability to cross-verify detected bladder events was enhanced, thereby reducing the FP rate and consequently, improving the classification accuracy. Incorporating this extra parameter allowed us to utilize a multimodal approach to validate detected contractions, distinguishing true contractions from motion artifacts to provide more reliable insights into bladder pressure changes in ambulatory settings.

Discussion

This study underscores the effectiveness of multimodal sensor fusion in bladder event detection, where we combined bladder pressure data with real-time movement activity to enhance the accuracy of detecting bladder events beyond what is achievable with single-channel measurements alone. By integrating activity data, this approach not only helped differentiate between true bladder contractions and motion-induced artifacts to reduce the FP rate but also provided insightful contextual information about bladder events. This distinction is particularly important for emerging sensors that measure P_{ves} alone and to analyze bladder pressure data from ambulatory subjects that are typically prone to significant P_{abd} artifacts.

Implementing optimized AR has the potential to improve real-time conditional stimulation in ambulatory settings by reducing FPs caused by patient movement. This study focused on optimizing the AR process by reducing the feature space and down-sampling the data with minimal accuracy loss, thereby decreasing the computational overhead required for

activity classification. While the AR experiments could be simplified to classify “at rest” or “motion,” the inclusion of specific movements such as walking and running, despite potential differences in gait between humans and pigs, is crucial. These activities are generic enough to capture basic motion patterns rather than specific behaviors unique to humans. Moreover, to evaluate the significance of individual features, we ran feature importance across all trials over 20 iterations. This process helped to identify consistently important features and provided a more robust estimate of feature importance. Additionally, the biomechanical differences are less significant in the context of this study, where the primary objective was to optimize AR process and leverage a multimodal sensor fusion approach to enhance the accuracy of bladder event detection systems in ambulatory settings with eventual application to human studies. A notable challenge encountered in this research involved synchronizing activity timestamps with bladder pressure data. Incompatibilities between the timestamps of these data streams led to the exclusion of one experiment from analysis, as the misalignment would lead to incorrect event classification. In the future, expanding this work to larger datasets and human studies will provide valuable insights to further enhance optimization strategies for both AR and bladder event detection in low-power bladder pressure monitoring implants. Moreover, we aim to expand our study to investigate the integration of similar sensor technologies such as a volume sensor with pressure and activity detection to improve patient monitoring and real-time conditional stimulation using wireless sensors in long-term ambulatory settings.

Conclusions

AR is crucial in personalized healthcare, enhancing the reliability of bladder event detection by providing contextual information, identifying motion artifacts, and reducing false positives in ambulatory settings. This study focused on optimizing AR through advanced feature reduction techniques and machine learning to minimize computational demands while maintaining accuracy. Our methods were validated using the HAR dataset consisting of 561 features and further applied to IMU data from an ambulating Yucatan minipig equipped with the UroMOCA device, achieving significant feature optimization with minimal accuracy loss. Furthermore, this study demonstrated the potential of multimodal sensor fusion in enhancing bladder event detection by integrating real-time movement activity with bladder pressure data. The integration of AR with ambulatory UDS can significantly enhance the accuracy of long-term diagnostics for LUTD by providing contextual data that helps distinguish between true bladder events and motion-induced artifacts. Additionally, AR may potentially be applied in neuromodulation strategies to reduce false positives in event classification systems, ensuring that electrical stimulation is administered precisely when true bladder contractions occur, thus improving the efficacy of treatments for LUTD. In the future, we aim to expand our work on larger datasets, human studies and explore additional approaches to enable on-chip activity tracking to improve wireless, catheter-free ambulatory bladder monitoring and treatment.

Funding

The author(s) disclosed receipt of the following financial support for the research, authorship, and/or publication of this article: Research reported in this publication was supported by the National Institutes of Health under award numbers OT2OD023873 and R56EB031042.

References

1. Gupta A, Defreitas G and Lemack GE. The reproducibility of urodynamic findings in healthy female volunteers: results of repeated studies in the same setting and after short-term follow-up. Neurourol Urodyn 2004; 23(4): 311–316. [PubMed: 15227647]
2. Scaldazza CV and Morosetti C. Effect of different sized transurethral catheters on pressure-flow studies in women with lower urinary tract symptoms. Urol Int 2005; 75(1): 21–25. [PubMed: 16037703]
3. Majerus SJ, Garverick SL, Suster MA, et al. Wireless, ultra-low-power implantable sensor for chronic bladder pressure monitoring. ACM JETC 2012; 8(2): 11. [PubMed: 26778926]
4. Majerus SJ, Hanzlicek B, Hacohen Y, et al. Wireless and catheter-free bladder pressure and volume sensor. IEEE Sens J 2024; 24(6): 7308–7316. [PubMed: 38500510]
5. Frainey BT, Majerus SJ, Derisavifard S, et al. First in human subjects testing of the uromonitor: a catheter-free wireless ambulatory bladder pressure monitor. J Urol 2023; 210(1): 186–195. [PubMed: 37293725]
6. Bourbeau DJ, Creasey GH, Sidik S, et al. Genital nerve stimulation increases bladder capacity after SCI: a meta-analysis. J Spinal Cord Med 2018; 41(4): 426–434. [PubMed: 28198657]
7. Bartley J, Gilleran J and Peters K. Neuromodulation for overactive bladder. Nat Rev Urol 2013; 10(9): 513–521. [PubMed: 23817408]
8. Majerus S, Basu AS, Makovey I, et al. Wireless bladder pressure monitor for closed-loop bladder neuromodulation. In: 2016 IEEE SENSORS, Orlando FL, USA. IEEE, 2016, pp. 1–3.
9. Majerus SJA, Offutt SJ, Brink TS, et al. Feasibility of real-time conditional sacral neuromodulation using wireless bladder pressure sensor. IEEE Trans Neural Syst Rehabil Eng 2021; 29: 2067–2075. [PubMed: 34606460]
10. Wright JP, Mughrabi IT, Wong J, et al. A fully implantable wireless bidirectional neuromodulation system for mice. Biosens Bioelectron 2022; 200: 113886. [PubMed: 34995836]
11. Mickle AD, Won SM, Noh KN, et al. A wireless closed-loop system for optogenetic peripheral neuromodulation. Nature 2019; 565(7739): 361–365. [PubMed: 30602791]
12. Karam R, Bhunia S, Majerus S, et al. Real-time, autonomous bladder event classification and closed-loop control from single-channel pressure data. In: 2016 38th Annual International Conference of the IEEE Engineering in Medicine and Biology Society (EMBC), Orlando, FL, USA. IEEE, 2016, pp. 5789–5792.
13. Anguita D, Ghio A, Oneto L, et al. "A public domain dataset for human activity recognition using smartphones," in The European Symposium on Artificial Neural Networks, 2013. [Online]. vailable: https://api.semanticscholar.org/CorpusID:6975432
14. Medtronic. Sacral neuromodulation using InterStim. http://professional.medtronic.com/pt/uro/snm/index.html. (accessed 2 April 2023).
15. Siegel SW, Catanzaro F, Dijkema HE, et al. Long-term results of a multicenter study on sacral nerve stimulation for treatment of urinary urge incontinence, urgency-frequency, and retention. Urology 2000; 56(6): 87–91.
16. Majerus S, Nguyen C, Brose S, et al. Automated closed-loop stimulation to inhibit neurogenic bladder overactivity. Proc IMechE, Part H: J Engineering in Medicine 2024; 238(6): 619–627.
17. Majerus S, Makovey I, Zhui H, et al. Wireless implantable pressure monitor for conditional bladder neuromodulation In: 2015 IEEE Biomedical Circuits and Systems Conference (BioCAS), Atlanta, GA, USA. IEEE, 2015, pp. 1–4.
18. McAdams I, Kenyon H, Bourbeau D, et al. Low-cost, implantable wireless sensor platform for neuromodulation research. In: 2018 IEEE Biomedical Circuits and Systems Conference (BioCAS), Cleveland, OH. IEEE, 2018, pp. 1–4.
19. Soebadi MA, Bakula M, Hakim L, et al. Wireless intravesical device for real-time bladder pressure measurement: study of consecutive voiding in awake minipigs. PLoS One 2019; 14(12): e0225821. [PubMed: 31790475]
20. Li C, Wu M, Liu J, et al. Noninvasive, wireless and real-time bladder pressure monitoring with biomimetic structured devices. Appl Mater Today 2022; 29: 101635.

21. Fletter PC, Majerus S, Cong P, et al. Wireless micromanometer system for chronic bladder pressure monitoring. In: 2009 Sixth International Conference on Networked Sensing Systems (INSS), Pittsburgh, Pennsylvania, USA. IEEE, 2009, pp. 1–4.
22. Majerus SJ, Fletter PC, Damaser MS, et al. Low-power wireless micromanometer system for acute and chronic bladder-pressure monitoring. IEEE Trans Biomed Eng 2010; 58(3): 763–767. [PubMed: 20934942]
23. Karam R, Bourbeau D, Majerus S, et al. Real-time classification of bladder events for effective diagnosis and treatment of urinary incontinence. IEEE Trans Biomed Eng 2015; 63(4): 721–729. [PubMed: 26292331]
24. Abbaraju V, Lewis K, and Majerus S. Machine learning for automated bladder event classification from single-channel vesical pressure recordings. In: 2022 IEEE Signal Processing in Medicine and Biology Symposium (SPMB), Philadelphia, Pennsylvania, USA. IEEE, 2022, pp. 1–6.
25. Deimerly Y, Rey P, Robert P, et al. Electromechanical damping in mems accelerometers: A way towards single chip gyrometer accelerometer co-integration. In: 2014 IEEE 27th International Conference on Micro Electro Mechanical Systems (MEMS), San Francisco, CA, USA. IEEE, 2014, pp. 725–728.
26. Gao Y, Meng L, Tong J, et al. Design and simulation of a novel single-chip integrated mems accelerometer gyroscope. Electronics 2022; 11(15): 2451.
27. Mannini A and Sabatini AM. Machine learning methods for classifying human physical activity from on-body accelerometers. Sensors 2010; 10(2): 1154–1175. [PubMed: 22205862]
28. Yang C-C and Hsu Y-L. A review of accelerometry-based wearable motion detectors for physical activity monitoring. Sensors 2010; 10(8): 7772–7788. [PubMed: 22163626]
29. Gjoreski H, Lustrek M, and Gams M, Accelerometer placement for posture recognition and fall detection, in 2011 Seventh International Conference on Intelligent Environments, Nottingham, UK. IEEE, 2011, pp. 47–54.
30. Taraldsen K, Chastin SF, Riphagen II, et al. Physical activity monitoring by use of accelerometer-based body-worn sensors in older adults: a systematic literature review of current knowledge and applications. Maturitas 2012; 71(1): 13–19. [PubMed: 22134002]
31. Jin C, De-Lin L, and Fen-Xiang M. An improved id3 decision tree algorithm. In: 2009 4th International Conference on Computer Science & Education, Nanning, China. IEEE, 2009, pp. 127–130.
32. Leutheuser H, Schuldhaus D and Eskofier BM. Hierarchical, multi-sensor based classification of daily life activities: comparison with state-of-the-art algorithms using a benchmark dataset. PLoS One 2013; 8(10): e75196. [PubMed: 24130686]
33. Chavarriaga R, Sagha H, Calatroni A, et al. The opportunity challenge: a benchmark database for on-body sensor-based activity recognition. Pattern Recognit Lett 2013; 34(15): 2033–2042.
34. Reiss A and Stricker D. Introducing a new benchmarked dataset for activity monitoring. In: 2012 16th International Symposium on Wearable Computers, Newcastle, UK. IEEE, 2012, pp. 108–109.
35. Reyzin L Boosting on a budget: Sampling for feature-efficient prediction. In: Proceedings of the 28th International Conference on Machine Learning (ICML-11), Bellevue, Washington, USA, 2011, pp. 529–536.
36. Elsts A, McConville R, Fafoutis X, et al. On-board feature extraction from acceleration data for activity recognition. In: Proceedings of the 2018 International Conference on Embedded Wireless Systems and Networks, Madrid, Spain. Junction Publishing, 2018, p. 163–168.
37. Challa SK, Kumar A and Semwal VB. A multibranch CNN-BiLSTM model for human activity recognition using wearable sensor data. Visual Comput 2022; 38(12): 4095–4109.
38. Chen Y, Guo M, and Wang Z. An improved algorithm for human activity recognition using wearable sensors. In: 2016 Eighth International Conference on Advanced Computational Intelligence (ICACI), Chiang Mai, Thailand, IEEE, 2016, pp. 248–252.
39. Vidya B and Sasikumar P. Wearable multi-sensor data fusion approach for human activity recognition using machine learning algorithms. Sens Actuators A Phys 2022; 341: 113557.
40. Deegalla S and Bostrom H. Reducing high-dimensional data by principal component analysis vs. random projection for nearest neighbor classification. In: 2006 5th International Conference on Machine Learning and Applications (ICMLA 06), Orlando, FL, IEEE, 2006, pp. 245–250.

41. Rogers J and Gunn S. Identifying Feature Relevance Using a Random Forest. In: International Statistical and Optimization Perspectives Workshop, Bohinj, Slovenia, Springer, 2005, pp. 173–184.

42. Anguita D, Ghio A, Oneto L, et al. Human activity recognition on smartphones for mobile context awareness. In: Advances in Neural Information Processing Systems 26: proceedings of the 2012 Conference, Lake Tahoe, Nevada, USA, 2012, pp. 1–9.

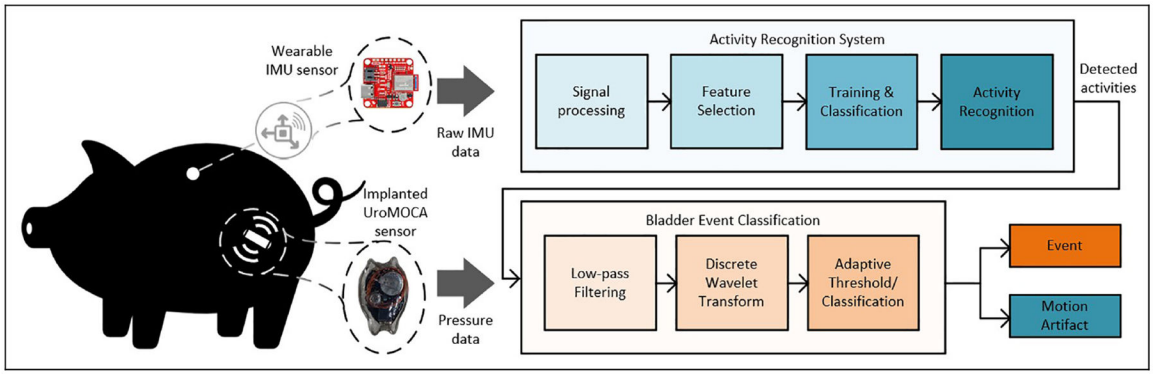

Figure 1.

Overview of the methodology. Simultaneous pressure and IMU recordings were collected from an ambulating Yucatan minipig subject.

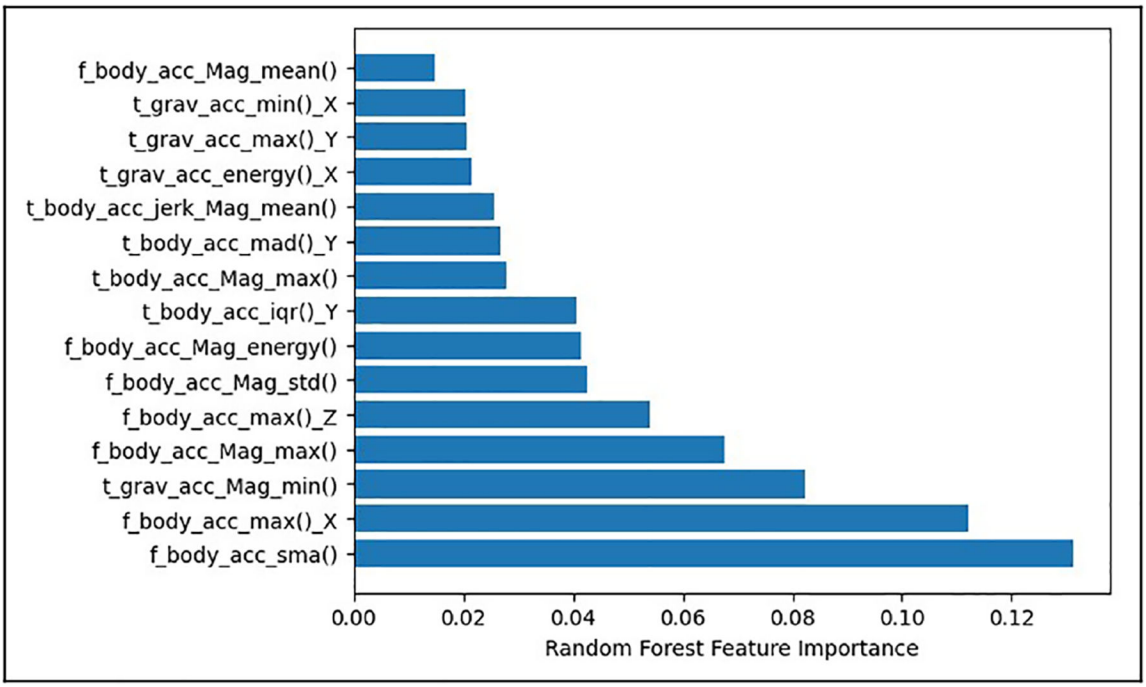

Figure 2.

Top 15 features identified by the random forest feature importance technique across all trials in the pig dataset, identified by time/frequency (*t*/*f*) domain, body/gravity components, axis (*x*, *y*, *z*) or magnitude, and function (e.g., maximum, minimum, mean, etc., out of which top 10 were used for activity classification.).

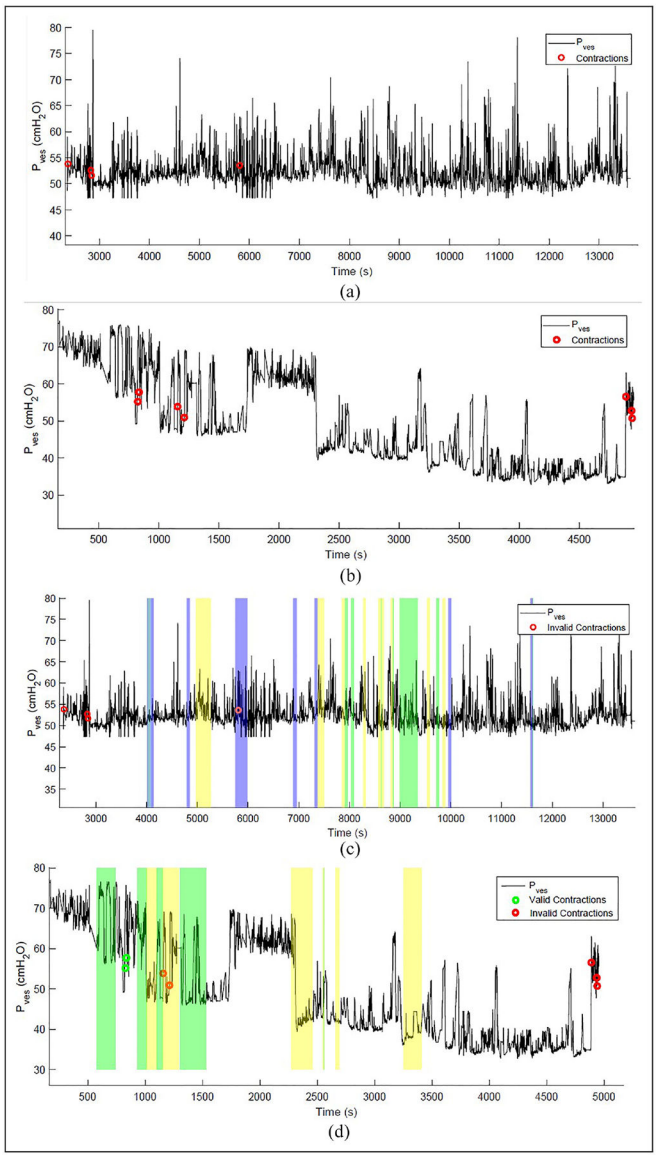

Figure 3.

(a) Contraction events detected in Experiment 1 (pressure-only) displaying only the bladder pressure data with contractions identified, without considering activity data. (b) Similar to (a), showing detected contractions without activity integration for Experiment 2. (c) Validated events in Experiment 1 with activity integration: Incorporating activity data, differentiating between valid and invalid contractions. Events categorized as invalid occur during activity periods. (d) Similar to (c) for Experiment 2. The color regions in (c) and (d) represent different activities: green for “WK” (walking), yellow for “ST” (standing/stationary), and blue for “RN” (running).

Table 1.

Computational complexity and cost assessment for feature extraction from time and frequency domains. This table lists signal processing features, their formulas, and operational definitions, alongside a breakdown of the computational operations required (addition, multiplication, division, square root, comparison, FFT) and an estimation of their relative computational cost ranging from very low to high.

Feature	Formula	Definition	Add	Mul	Div	Sqrt	Comp	FFT	Cost
min(s)	$\min_i(s_i)$	Minimum value	–	–	–	–	n	–	Very low
max(s)	$\max_i(s_i)$	Maximum value	–	–	–	–	n	–	Very low
mean(s)	$\frac{1}{n}\sum_{i=1}^{n} s_i$	Average value	$n-1$	–	1	–	–	–	Low
std(s)	$\sqrt{\frac{1}{n-1}\sum_{i=1}^{n}(s_i-\bar{s})^2}$	Standard deviation	$2n-1$	n	1	1	–	–	Medium
correlation(s)	$\frac{\mathrm{cov}(X,Y)}{\sigma_x\sigma_y}$	Pearson correlation coefficient	$4n$	$3n+1$	1	–	–	–	Medium
energy(s)	$\sum_{i=1}^{n}(s_i)^2$	Sum of squares	$n-1$	n	–	–	–	–	Medium
entropy(s)	$-\sum_{i=1}^{n} p(s_i)\log_2 p(s_i)$	Signal unpredictability	$n-1$	n	–	–	–	–	High
skewness(f)	skew(f)	Skewness	$2n$	$2n$	1	–	–	$6n\log_2 n$	High
kurtosis (f)	kurtosis(f)	Kurtosis	$2n$	$2n$	1	1	–	$6n\log_2 n$	High
bandsEnergy(f)	bandsEnergy(f)	Energy in a frequency interval	$14m$	$14m$	–	–	–	$6n\log_2 n$	High

Table 2.

Results of classifiers on the HAR dataset with feature size n = 50, using features identified by principal component analysis (PCA), random forests (RF), and random projections (RP), with classifiers Gaussian Naïve Bayes (GB) and logistic regression (LR).

Technique	Classifier	Accuracy (%)	F1-score
PCA	GB	87.8	0.88
	LR	93.9	0.94
RF	GB	87.1	0.88
	LR	93.9	0.94
RP	GB	87.3	0.87
	LR	93.8	0.94

Table 3.

Results of activity classification in pig dataset using logistic regression (LR) for varying sampling frequencies (F_s).

Exp.	Trials	(F_s)	Accuracy	F1-score
P1		100	96.8	0.97
	2	50	92.2	0.91
		25	88.1	0.87
P2		100	95.4	0.95
	1	50	90.1	0.89
		25	83.9	0.83
P3		100	96.9	0.97
	2	50	92.3	0.92
		25	88.5	0.88

Table 4.

Confusion matrix of the detected and verified activities for all experiments in the pig dataset.

Experiment	Trials	Activity		T’	F’
P1	2	WK	T	11	1
			F	1	11
		RN	T	8	1
			F	1	8
		ST	T	13	1
			F	1	13
P2	1	WK	T	3	1
			F	1	3
		RN	T	1	0
			F	0	1
		ST	T	1	1
			F	1	1
P3	2	WK	T	6	1
			F	1	6
		ST	T	10	2
			F	2	10

Activities include Walk (WK), Run (RN) and Stand (ST).

Table 5.

Results of bladder event detection with integrated activity data.

Experiment	Trials	Total detected events	Valid events (w activity verification)	Correctly classified (pressure)(%)	Correctly classified (pressure + activity) (%)
P1	2	12	8	82	90
P3	2	8	7	80	87
Average classification				81	89